

¹ Research Paper/

² FloPy Workflows for Creating and Constructing
³ Structured and Unstructured MODFLOW 6 Models

⁴ Joseph D. Hughes^{1,*}, Christian D. Langevin², Scott R. Paulinski³, Joshua D.
⁵ Larsen⁴, and David Brakenhoff⁵

⁶ ¹U.S. Geological Survey, Integrated Modeling and Prediction Division, 927 W Belle Plaine Ave,
⁷ Chicago, IL, USA

⁸ ²U.S. Geological Survey, Integrated Modeling and Prediction Division, 2280 Woodale Dr, Mounds
⁹ View, MN, USA

¹⁰ ³U.S. Geological Survey, California Water Science Center, 3130 Skyway Drive, Suite 602, Santa
¹¹ Maria, CA, USA

¹² ⁴U.S. Geological Survey, California Water Science Center, 6000 J Street, Placer Hall, Sacramento,
¹³ CA, USA

¹⁴ ⁵Artesia Water, Korte Weistraat 12, Schoonhoven, Netherlands

¹⁵*Corresponding author jdhughes@usgs.gov

¹⁶ April 13, 2023

¹⁷ **Abstract**

¹⁸ FloPy is a Python package for creating, running, and post-processing MODFLOW-based
¹⁹ groundwater flow and transport models. FloPy functionality has expanded to support
²⁰ the latest version of MODFLOW (MODFLOW 6) including support for unstructured
²¹ grids. FloPy can simplify the process required to download MODFLOW-based and other

22 executables for Linux, MacOS, and Windows operating systems. Expanded FloPy
23 capabilities include (1) full support for structured and unstructured spatial
24 discretizations; (2) geoprocessing of spatial features and raster data to develop model
25 input for supported discretization types; (3) the addition of functionality to provide
26 direct access to simulated output data; (4) extension of plotting capabilities to
27 unstructured MODFLOW 6 discretization types; and (5) the ability to export model
28 data to shapefiles, NetCDF, and VTK formats for processing, analysis, and visualization
29 by other software products. Examples of using expanded FloPy capabilities are
30 presented for a hypothetical watershed. An unstructured groundwater flow and transport
31 model, with several advanced stress packages, is presented to demonstrate how FloPy
32 can be used to develop complicated unstructured model datasets from original source
33 data (shapefiles and rasters), post-process model results, and plot simulated results.

34 Introduction

35 FloPy is a Python package for constructing, running, and post processing MODFLOW-based
36 groundwater flow and transport models ([Bakker et al. 2016](#)). It is open-source and developed
37 by a growing community of contributors. The combination of open-source programming
38 languages (such as Python) with version control software (such as Git) allows the model
39 construction process to be documented, reproducible, and easily inspected and used by others.
40 This workflow has been recommended as one way to facilitate repeatable research and sharing
41 of ideas ([Fienen and Bakker 2016](#)). Bakker et al. (2016) describe the general approach for
42 working with models within the Python environment and emphasize the reproducible nature
43 of developing models through scripting.

44 FloPy has been used to pioneer new methods and analysis tools, such as deep learning
45 approaches for improving groundwater model calibration ([Sun 2018; Zhou and Tartakovsky
46 2021](#)), regionalizing residence times using metamodeling ([Starn and Belitz 2018](#)), applying
47 iterative ensemble approaches for calibration and uncertainty quantification ([White 2018](#)), and
48 exploring alternative parameterization schemes for risk analysis ([Knowling et al. 2019](#)). There

49 are numerous examples of constructing MODFLOW models with FloPy to solve applied
50 groundwater problems (Befus et al. 2017; van Engelen et al. 2018; Ebeling et al. 2019; Zipper
51 et al. 2019; Befus et al. 2020). FloPy is also being used in other software and workflows to
52 improve repeatability and robustness through automated model construction (White et al.
53 2020; Fienen et al. 2022; Larsen et al. 2022; Leaf and Fienen 2022). FloPy is also used in
54 GIS-based tools, such as FREEWAT (Rossetto et al. 2018) and other cyberinfrastructures
55 (Essawy et al. 2018) to export models into MODFLOW datasets. FloPy can also be used as
56 the “glue” to help couple MODFLOW to other hydrological models (Burek et al. 2020) or, for
57 example, to agent-based models designed to quantify the effects of decision makers on
58 environmental behavior (Jaxa-Rozen et al. 2019).

59 The U.S. Geological Survey uses FloPy to teach MODFLOW and groundwater modeling
60 to early- and mid-career engineers and scientists. Other organizations also use FloPy to teach
61 MODFLOW (e.g., Australian Water School 2023; Hatari Labs 2023). We routinely rely on
62 FloPy to load and help identify problems in user model applications, and with the initial
63 release of the MODFLOW 6 groundwater flow model (Langevin et al. 2017), we started to rely
64 on FloPy to help with development of the MODFLOW program. We write tests that rely on
65 FloPy to construct and run models, and then read output. We then verify that the output is
66 as expected, by using analytical solutions, other models, or results that have been confirmed
67 to be correct.

68 The purpose of this paper is to highlight FloPy new functionality for creating and
69 constructing structured and unstructured MODFLOW models. We provide examples that
70 demonstrate these new capabilities, and reinforce the advantages of the modern scripting
71 workflow for developing reproducible structured and unstructured MODFLOW groundwater
72 flow and transport models that can be updated as new data become available. The examples
73 also demonstrate workflows that develop different model grids for the same model domain.
74 The important advances described here include (1) complete support for all models, packages,
75 and options implemented in the core version of MODFLOW supported by the U.S. Geological
76 Survey (Hughes et al. 2017; Langevin et al. 2017; Provost et al. 2017; Langevin et al. 2020;

77 Morway et al. 2021; Langevin et al. 2022; Hughes et al. 2022; Mancewicz et al. 2022); (2)
78 generalized support for models based on a structured grid consisting of layers, rows, and
79 columns, and also for models based on unstructured grids; (3) implementation of new
80 geoprocessing capabilities to rapidly populate models with data from a variety of input
81 sources; (4) simplified access to model results; (5) plotting capabilities for map and
82 cross-section views of model data; and (6) export capabilities for writing model data to a
83 variety of output formats.

84 FloPy Support for MODFLOW 6

85 The most recent version of MODFLOW (MODFLOW 6) is an object-oriented program and
86 framework developed to provide a platform for supporting multiple models and multiple types
87 of models within the same simulation (Hughes et al. 2017). These models can be independent
88 of one another with no interaction, they can exchange coefficients and dependent variables
89 (*e.g.*, head), or they can be tightly coupled at the matrix level by adding them to the same
90 numerical solution. Transfer of information between models is isolated to exchange objects,
91 which allow models to be developed and used independently. Within this new framework, a
92 regional-scale groundwater model may be coupled with multiple local-scale groundwater
93 models.

94 MODFLOW 6 currently includes the Groundwater Flow (GWF) Model and the
95 Groundwater Transport (GWT) Model each with packages to represent surface water
96 processes, groundwater extraction, external boundaries, mass sources and sinks, and mass
97 sorption and reactions. GWF and GWT models can be developed using structured model
98 grids consisting of layers, rows, and columns or they can be developed using more general
99 unstructured grids using many of the concepts and numerical approaches available in
100 MODFLOW-USG (Panday et al. 2013). MODFLOW 6 also includes advanced formulations to
101 simulate three-dimensional anisotropy and dispersion (Provost et al. 2017), coupled

102 variable-density groundwater flow and transport ([Langevin et al. 2020](#)), and a water mover
103 package to represent natural and managed hydrologic connections ([Morway et al. 2021](#)).

104 Development and testing of the MODFLOW 6 program relies heavily on tight integration
105 with FloPy. A key component of this tight integration is the capability to quickly support new
106 MODFLOW 6 models and packages with FloPy. Unlike the FloPy support for previous
107 MODFLOW versions (*e.g.*, MODFLOW-2005, MODFLOW-NWT, MODFLOW-USG, and
108 SEAWAT), the FloPy Python classes for MODFLOW 6 are dynamically generated from
109 simple text files, called “definition files,” that describe the input file structure. All
110 MODFLOW 6 model input files are described using these definition files. This allows
111 MODFLOW 6 developers to write tests for new models, packages, and functionality as they
112 are developed. These definition files are used to programmatically generate the user input and
113 output guide for MODFLOW 6. These same definition files are also used to generate FloPy
114 classes, with documentation corresponding to input variable descriptions in the input and
115 output guide. New functionality can be added by users to existing packages by modifying
116 existing definition files. The existing definition files can also be used as a template for creating
117 classes for new MODFLOW 6 models or packages.

118 Common Modeling Tasks

119 The code snippets presented in this section that demonstrate how to create model grids,
120 geoprocess data, process output, plot model data, and export model data are available as
121 Jupyter notebooks ([Kluyver et al. 2016](#)) at the internet addresses indicated in the [Summary](#)
122 and [Conclusions](#) section.

123 Getting MODFLOW and Other Related Executables

124 FloPy for MODFLOW 6 relies on a number of helper classes, which wrap functionality
125 available in pre-compiled external utility programs, to generate unstructured models and
126 calculate water budgets on user-defined zones. These external utility programs (*e.g.*,

127 GRIDGEN, Triangle, ZONEBUDGET, etc.), MODFLOW 6, and other MODFLOW-related
128 programs (*e.g.*, MODPATH, MT3DMS, MT3D-USGS, SEAWAT, etc.) can be installed using

129 `get-modflow :flopy`

130 in a terminal or at the command line after installing FloPy. The `get-modflow` command
131 detects the operating system (Linux, MacOS, or Windows) and downloads the latest
132 operating-system-specific release of MODFLOW and related programs from an [Executables](#)
133 [GitHub repository](#). `get-modflow` can also download previous versions of MODFLOW 6 and
134 the latest development version of MODFLOW 6 using instructions available on the [FloPy](#)
135 [GitHub repository](#).

136 Managing and Creating Model Grids

137 FloPy was originally developed to support models that are based on a structured grid
138 consisting of layers, rows, and columns. Recent support for unstructured grids in MODFLOW
139 ([Panday et al. 2013; Langevin et al. 2017](#)) required revisions to the underlying approach for
140 managing spatial discretization information in FloPy. Grid information is containerized into a
141 single location and used throughout FloPy modeling tasks for geospatial processing, plotting,
142 and exporting. Spatial discretization is now handled in FloPy through dedicated model grid
143 classes. There is a `Grid` class, which serves as the base class for the `StructuredGrid`,
144 `VertexGrid`, and `UnstructuredGrid` classes. Grid objects can be created by the user for
145 preprocessing, and they are automatically generated and attached to a FloPy model object.

146 Structured MODFLOW grids can have constant row and column spacings, as shown in
147 Figure 1A, or they can have variable row and column spacings to focus resolution around an
148 area of interest, as shown in Figure 1B. The following Python code shows how to create a
149 `StructuredGrid` object in FloPy. A `StructuredGrid` object can also be created from
150 discretization data required when instantiating a MODFLOW 6 `DIS` object using
151 `flopy.mf6.ModflowGwfdis()`.

```
152     >>> structured_grid = flopy.discretization.StructuredGrid(nlay=nlay,
153     ... delr=delr, delc=delc, xoff=0.0, yoff=0.0, angrot=0.0, top=top, botm=botm)
```

154 MODFLOW 6 was developed to support multi-model simulations (Hughes et al. 2017).

155 One form of multi-model simulation is a nested grid application in which a more finely
156 discretized child model is embedded within a more coarsely discretized parent model (Mehl
157 and Hill 2006; Vilhelmsen et al. 2012; Mehl and Hill 2013; Fienen et al. 2022). The use of a
158 locally refined grid (LGR) within an encompassing parent grid offers computational benefits in
159 that the additional refinement is targeted to an area of interest. FloPy provides a `Lgr()`
160 utility class for constructing the data required to tightly couple parent and child models
161 within a single MODFLOW 6 simulation. Figure 1C shows two `StructuredGrid` objects—one
162 object represents the parent model grid and the other represents the nested child grid. The
163 `Lgr()` utility class defines the connection properties between cells in the parent model and
164 cells in the child model. Connection properties consist of distances, areas, and other geometric
165 information needed to calculate flow between cells in different models. The `Lgr()` utility class
166 is general in that the child model can have more layers than the parent model. The following
167 Python code shows the steps for creating a child `StructuredGrid` object using data for the
168 parent grid with the `Lgr()` utility class.

```
169     idomain_parent = np.ones((nlay_parent, nrow_parent, ncol_parent), dtype=int)
170     idomain_parent[0, 8:12, 13:18] = 0
171     ncpp, ncppl = 3, [1]
172     lgr = Lgr(nlay_parent, nrow_parent, ncol_parent,
173                 delr_parent, delc_parent, topparent, botmparent,
174                 idomain_parent, ncpp=ncpp, ncppl=ncppl,
175                 xllp=0.0, yllp=0.0)
176     delr, delc = lgr.get_delr_delc()
177     xoff, yoff = lgr.get_lower_left()
```

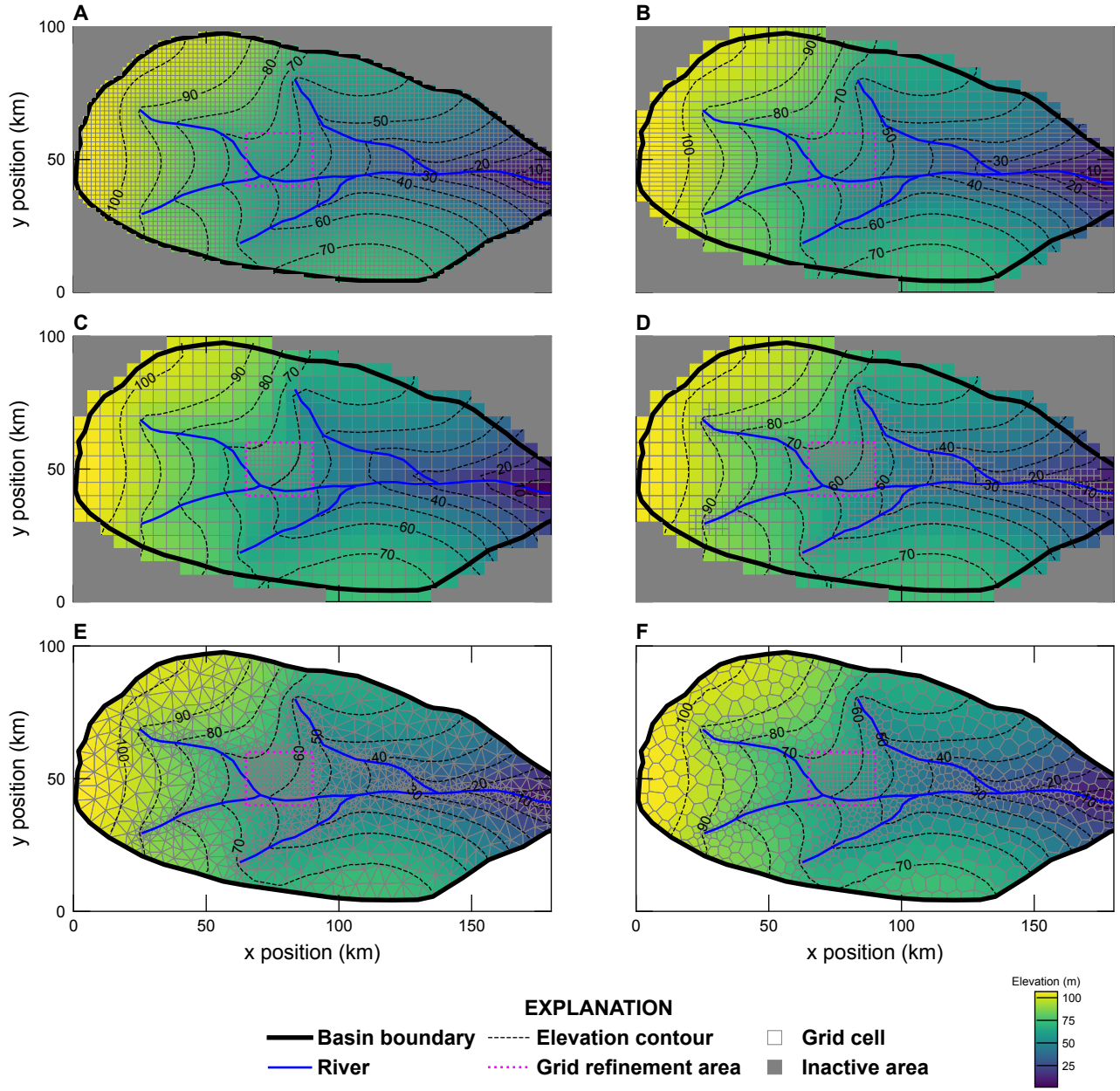


Figure 1: Examples of grids that can be generated and processed using FloPy for a hypothetical watershed, including (A) a structured MODFLOW grid with constant and equal row and column spacings, (B) a structured MODFLOW grid with variable row and column spacings, (C) a structured MODFLOW child grid nested within a structured MODFLOW parent grid, (D) a quadtree grid generated with the GRIDGEN program (Lien et al. 2014) through the FloPy wrapper, (E) a triangular grid generated with the Triangle program (Shewchuk 1996) through the FloPy wrapper, and (F) a Voronoi grid created from the triangular mesh. All of the grids have refinement in the location of the child grid in (C).

```
178     structured_gridchild = StructuredGrid(delr=delr, delc=delc,  
179                                         xoff=xoff, yoff=yoff)
```

180 The child grid is created in the inactive area of the parent grid (`idomain_parent`) and the
181 returned `lgr` object contains all of the information required to create a child `StructuredGrid`
182 object. The connection properties needed to create the MODFLOW 6 Exchange input file for
183 the parent and child grids can be retrieved using `lgr.get_exchange_data()`.

184 FloPy supports management and generation of unstructured grids. Unstructured grids
185 are represented as layered or fully unstructured. A layered grid is one in which the same grid
186 applies to all model layers. An unstructured grid is more general and allows the model grid to
187 change with depth. Layered grids and unstructured grids are stored in FloPy as `VertexGrid`
188 and `UnstructuredGrid` objects, respectively.

189 Layered quadtree grids can be created using the `Gridgen()` utility class, which is a
190 wrapper around the GRIDGEN program (Lien et al. 2014). GRIDGEN starts with a
191 structured MODFLOW grid with constant and equal row and column spacing defined by the
192 user. The program then recursively subdivides individual cells that intersect with refinement
193 features into quarters until a maximum level of refinement is met. Refinement features may be
194 points, lines, or polygons. Smoothing is automatically handled so that a cell is connected to
195 no more than two cells in any primary horizontal direction and four cells in the vertical
196 direction. Figure 1D shows an example of a quadtree grid created with GRIDGEN in which a
197 base grid is refined two levels along streams and in the grid refinement area shown in Figure 1.
198 The following Python code shows the steps for creating the quadtree grid with GRIDGEN.

```
199     sim = flopy.mf6.MFSimulation()  
200     gwf = flopy.mf6.ModflowGwf(sim)  
201     dis6 = flopy.mf6.ModflowGwfdis(gwf, nrow=nrow, ncol=ncol, delr=dy, delc=dx)  
202     g = Gridgen(dis6, model_ws=temp_path)  
203     g.add_refinement_features([[lgr_polygon_xy]], "polygon", 2, range(1))
```

```

204     g.add_refinement_features(stream_points, "line", 2, range(1))
205
206     g.build(verbose=False)
207
208     gridprops_vg = g.get_gridprops_vertexgrid()
209
210     quadtree_grid = flopy.discretization.VertexGrid(**gridprops_vg)

```

208 FloPy also provides a wrapper utility for the Triangle mesh generation program
 209 ([Shewchuk 1996](#)). The `Triangle()` utility class writes the Triangle program input file, runs
 210 the Triangle program, and then loads the triangular mesh. Users provide the maximum area
 211 for individual triangles, angle constraints, a polygon describing the model domain, and so
 212 forth. Figure 1E shows an example of a triangular grid created with the Triangle program.
 213 The Python code for creating the triangular grid is shown below.

```

214     tri = flopy.utils.triangle.Triangle(maximum_area=maximum_area,
215                                         angle=30, nodes=refinement_verts,
216                                         model_ws=temp_path)
217
218     tri.add_polygon(boundary_points)
219
220     tri.build(verbose=False)
221
222     cell2d = tri.get_cell2d()
223
224     vertices = tri.get_vertices()
225
226     triangular_grid = VertexGrid(vertices=vertices, cell2d=cell2d,
227                                   idomain=idomain, nlay=nlay, ncpl=tri.ncpl,
228                                   top=top, botm=botm)

```

224 `refinement_verts` in the triangular grid code shown above contains the user-specified stream
 225 vertices and the horizontal cell vertices for the grid refinement area shown in Figure 1.

226 A triangular grid can be converted by FloPy into a Voronoi grid using the
 227 `VoronoiGrid()` utility class. The `VoronoiGrid()` utility class uses SciPy routines ([Virtanen et al. 2020](#)) to construct Voronoi polygons around each vertex in the triangular mesh. Figure

229 1F shows an example of a Voronoi grid created from the triangular mesh shown in Figure 1E.
230 The steps for creating the Voronoi grid from the previously created `Triangle()` object (`tri`)
231 are shown below.

```
232     vor = flopy.utils.voronoi.VoronoiGrid(tri)  
233     gridprops = vor.get_gridprops_vertexgrid()  
234     voronoi_grid = VertexGrid(**gridprops, nlay=nlay, idomain=idomain)
```

235 The `StructuredGrid`, `VertexGrid`, and `UnstructuredGrid` classes have useful properties
236 and methods for accessing or mapping locations on the model grid including: (1) converting x,
237 y pairs from local to global coordinates (`.get_coords()`) and from global to local coordinates
238 (`.get_local_coords()`); (2) getting x, y, and z coordinates for cell centers (`.xcellcenters`,
239 `.ycellcenters`, `.zcellcenters`, and `.xyzcellcenters`) and vertices (`.xvertices`,
240 `.yvertices`, `.zvertices`, and `.xyzvertices`); and (3) intersecting a list of x, y pairs with
241 the grid and returning the appropriate `cellid` (`.intersect()`). Local coordinates are
242 model-based coordinates and global coordinates are coordinates generated after transforming
243 local model coordinates using user-specified x-offset, y-offset, and rotation angle values; global
244 coordinates are equal to local coordinates if the x-offset, y-offset, and rotation angle are all
245 zero. Other useful grid class properties and methods include generating a grid object from a
246 MODFLOW 6 binary grid file (`.from_binary_grid_file()`), retrieving cell thicknesses
247 (`.cell_thickness`), and calculating the saturated thickness for each cell by passing a head
248 array with dimensions consistent with the grid object (`.saturated_thickness(head)`).

249 The new FloPy capabilities for generating and testing different types of model grids
250 allows for innovation in the way a study area is discretized. For example, [Guira \(2018\)](#) used a
251 Voronoi grid to add additional resolution in the vicinity of irrigation wells in the Frenchman
252 Creek Basin in Nebraska, USA to quantify the effects of land-use change and irrigation on
253 streamflow depletion. Furthermore, the ability to develop multi-model simulations using
254 FloPy allows higher-resolution inset models to be added in focused areas. [Fienen et al. \(2022\)](#)

255 used local grid refinement models tightly coupled to inset models that were in turn loosely
256 coupled to a coarse regional model, to better represent lakes and quantify the effects of distant
257 pumping on lake and groundwater interactions in the Central Sands region in Wisconsin,
258 USA. The inset groundwater flow models with lakes (Fienen et al. 2022) were developed using
259 `modflow-setup` (Leaf and Fienen 2022), which relies on FloPy to generate MODFLOW 6
260 datasets.

261 Geospatial Processing

262 Geospatial processing is often a fundamental part of creating a groundwater model. New
263 geospatial processing functionality has been added to FloPy to help users construct models
264 using data from common input sources. The geospatial processing functionality has been
265 implemented to work with the different types of model grids so that it is straightforward to
266 build and construct models with different grid resolutions or grid types. The geospatial
267 processing routines work with all three of the model grid types (`StructuredGrid`,
268 `VertexGrid`, and `UnstructuredGrid`).

269 A common geospatial processing task is resampling of raster data onto a model grid. For
270 example, it is often necessary as part of model construction to resample a raster data set of
271 land surface elevation onto a model grid. FloPy includes a new raster sampling utility based
272 on the Rasterio Python package (Gillies et al. 2013). The following Python code demonstrates
273 the steps for resampling an Esri ASCII raster format grid onto a Voronoi grid.

```
274     fine_topo = flopy.utils.Raster.load("./grid_data/fine_topo.asc")  
275     top_vg = fine_topo.resample_to_grid(voronoi_grid, band=fine_topo.bands[0],  
276                                         method="linear", extrapolate_edges=True)
```

277 The result of raster resampling is a NumPy array, equal in size to the number of cells in one
278 layer of the Voronoi grid. The NumPy array contains an interpolated land surface elevation
279 for each model cell. In this Python code example, the land surface grid was interpolated to the

280 Voronoi grid using a “linear” method, however, the method also supports “nearest”, “cubic”,
281 and other options (“mean”, “median”, “mode”, “min”, and “max”) available in the rasterstats
282 Python package (Perry 2013) for geostatistical resampling. Elevation ranges in Figure 1 show
283 the results of linear raster resampling for land surface onto a variety of structured and
284 unstructured model grids.

285 Performing intersections of hydrologic features with the model grid is another common
286 modeling task. FloPy is now equipped with robust and efficient capabilities for intersecting a
287 model grid with points, lines, and polygons. The underlying intersection routines rely on the
288 Shapely Python package (Gillies 2022) to determine intersection properties. When a point or
289 collection of points is intersected with a model grid, the grid intersection routine returns the
290 cells that intersect with the points. When a line or collection of lines is intersected with a
291 model grid, the grid intersection routine returns the cells that intersect with the lines and the
292 lengths of lines within each intersected cell. The line and grid intersection routine also creates
293 and returns individual line segments of the line features within each intersected cell. When a
294 polygon or collection of polygons is intersected with a model grid, the grid intersection routine
295 returns the cells that intersect with the polygons and the polygon area within the cell. The
296 polygon and grid intersection routine also creates and returns individual polygons of the
297 original polygon features within each intersected cell.

298 The following Python code demonstrates the steps for identifying the grid cells that
299 intersect with a collection of line segments.

```
300     ixs = flopy.utils.GridIntersect(voronoi_grid)
301
302     results = []
303
304     for points in segments:
305         segment = ixs.intersect(LineString(points))
306
307         results.extend(segment["cellids"].tolist())
```

305 The result of this code snippet (`results`) is a list of Voronoi grid cell numbers that intersect

306 with the line segments. The `ixs.intersect()` method also returns the "lengths" of the
307 shapely collection intersecting each cell, the "vertices" corresponding to each cell that
308 intersects a collection of shapely objects, and a shapely object ("ixshape") for each portion
309 of the original shape (`LineString(points)`) that intersects a cell. Results of the grid
310 intersection for a linear stream network and the six different model grids is shown in Figure 2.

311 Processing MODFLOW 6 output

312 MODFLOW 6 has many different types of output that can be created during a simulation. A
313 GWF model, for example, can write simulated heads and detailed budget information to
314 binary files. Global model budgets are written to standard MODFLOW listing (*.lst) files
315 and can be written to comma-separated value text files. Some individual GWF and GWT
316 model advanced stress packages can also write simulated output. Advanced packages solve
317 their own continuity equation and include the Lake (LAK), Streamflow Routing (SFR),
318 Multi-Aquifer Well (MAW), Unsaturated Zone Flow (UZF), and Mover (MVR) packages. For
319 example, the LAK Package can write simulated lake stages and detailed lake budget
320 information to binary files. Likewise, the MAW Package can write simulated well head and
321 well budgets to binary files. Recent improvements have been made to FloPy to allow users
322 easier access to simulation results using `.output` routines available for MODFLOW 6 models
323 and advanced stress packages. Prior to these improvements, users were required to instantiate
324 head, concentration, and budget file readers using file paths and names in order to access
325 simulation results. With the `.output` routines, the file readers are automatically generated
326 when called by the user.

327 The following `.methods()` syntax shows how a user can discover the type of output
328 information that is available for the specified `gwf` model.

```
329     >>> gwf.output.methods()  
330     ['list()', 'zonebudget()', 'budget()', 'budgetcsv()', 'head()']
```

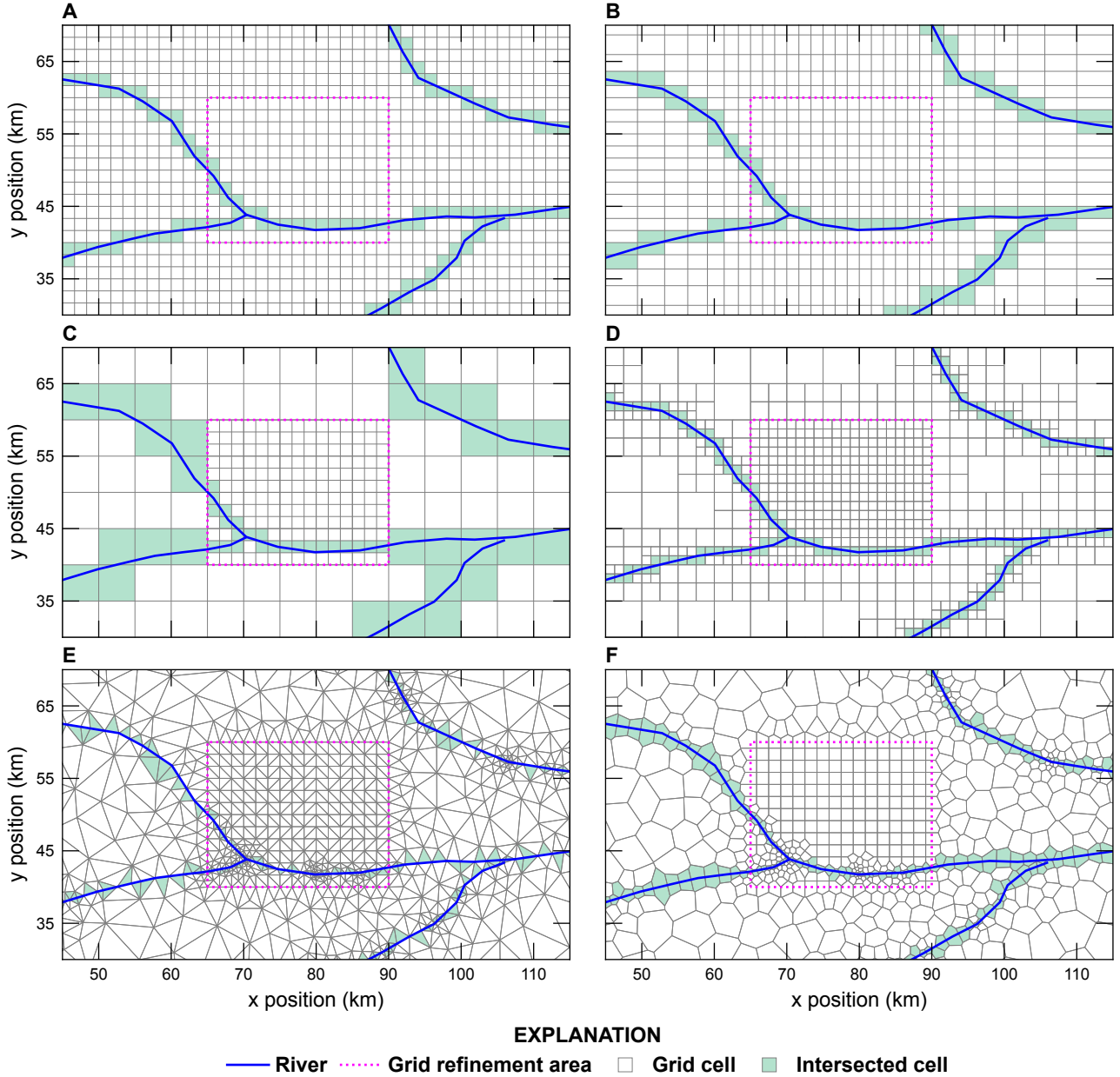


Figure 2: Examples of the intersection of a linear stream network with the model grids shown in Figure 1. Intersections were performed using FloPy for (A) a structured MODFLOW grid, (B) a structured MODFLOW grid with variable row and column spacing, (C) a structured MODFLOW child grid nested within a structured MODFLOW parent grid, (D) a quadtree grid, (E) a triangular grid, and (F) a Voronoi grid. Shaded cells represent those cells that intersect with the linear stream network.

331 The `.list()` method can be used to get the incremental (`incremental=True`) or cumulative
 332 budget information from the MODFLOW listing file for the `gwf` model for a user-specified

333 simulation time, zero-based time step and stress period tuple, or zero-based index. The
334 `.zonebudget()` method allows the user to build water and mass budgets for individual zones
335 for MODFLOW 6 models, run the ZONEBUDGET program, and access ZONEBUDGET
336 output. The `.budget()` method provides access to data in binary MODFLOW 6 cell-by-cell
337 budget files. The `.budgetcsv()` method provides access to cumulative and incremental global
338 budgets written by MODFLOW 6 to comma separated value files. The `.head()` method gives
339 user access to data in the binary MODFLOW 6 head file.

340 Similarly, the following `.methods()` syntax shows how a user can discover the type of
341 output information that is available for an advanced stress package, such as the LAK package.

```
342     >>> gwf.lak.output.methods()  
343     ['zonebudget()', 'budget()', 'budgetcsv()', 'package_convergence()', 'obs()',  
344      'stage()']
```

345 The `.package_convergence()` method can be used to get the convergence information for an
346 advanced stress package. The `.obs()` method can be used to get observation data saved for a
347 model or stress package as a NumPy record array or pandas data frame. The `.stage()`
348 method provides access to the dependent variable calculated by the LAK package and behaves
349 similarly to the `.head()` method for the `gwf` model.

350 Processing simulated dependent variables

351 Simulated output for dependent variables are written by MODFLOW 6 to binary files.
352 Simulated heads and concentrations written by the GWF and GWT models, respectively, can
353 be accessed using the `.output` method on the FloPy `gwf` or `gwt` objects. To access the
354 simulated head output, for example, a call can be made to the head file reader to retrieve data
355 for a specified simulation time using the `.get_data()` method as follows.

```
356     head = gwf.output.head().get_data(totim=1.0)
```

357 In this case, the `head` variable is retrieved for a user-specified simulation time (`totim=` and `is` a
358 NumPy array equal in size to the size of the model grid. Head data can also be accessed for a
359 zero-based time step–stress period tuple

```
360     head = gwf.output.head().get_data(kstpkper=(0,0))
```

361 or a zero-based index

```
362     head = gwf.output.head().get_data(idx=0)
```

363 Processing simulated cell-by-cell budgets

364 Similar to head output, cell-by-cell budget information can be accessed using FloPy. Unlike
365 the simulated head file, the cell-by-cell budget file can have data for more than one item and
366 these items may be stored in the file as arrays or lists of data. The data in the cell-by-cell
367 budget file can be determined using

```
368 >>> gwf.output.budget().list_unique_records()
```

```
369     RECORD           IMETH
```

```
370 -----
```

```
371     FLOW-JA-FACE      1
```

```
372     DATA-SPDIS       6
```

```
373     DATA-SAT         6
```

```
374     WEL               6
```

```
375     DRN               6
```

```
376     RCHA              6
```

```
377     EVTA              6
```

```
378     SFR               6
```

```
379     LAK               6
```

380 The IMETH code indicates if the data is stored in the file as an array (IMETH=1) or if it is list
381 based (IMETH=6). Cell-by-cell specific-discharge data can be extracted using

```
382     spdis = gwf.output.budget().get_data(totim=1.0, text="DATA-SPDIS")[0]
```

383 Simulated values for specific discharge for each cell are returned as a list containing a NumPy
384 record array for the user-specified simulation time (totim=). Like MODFLOW head data, all
385 of the data in the cell-by-cell data file for a user-specified simulation time (totim=), zero-based
386 time step and stress period tuple (kstp,kper=), or zero-based index (idx=) can also be
387 extracted. Simulated specific discharge information can be processed into a form that can be
388 plotted with FloPy using

```
389     qx, qy, qz = flopy.utils.postprocessing.get_specific_discharge(spdis, gwf,  
390                                         head=head)
```

391 The optional argument head= above sets the specific discharge in inactive or dry cells to a
392 value that will not be plotted.

393 Performing zone budget analyses

394 `zonebudget()` output methods are available for both the `gwf` model and the `gwf.lak`
395 advanced stress package examples shown above because they both solve a continuity equation.
396 Other flow and transport advanced stress packages (*e.g.*, SFR, Streamflow Transport (SFT),
397 Unsaturated Zone Flow (UZF), Unsaturated Zone Transport (UZT), MAW, and Multi-Aquifer
398 Well Transport (MWT)) also solve continuity equations and can be used with this zone
399 budget functionality. The `zonebudget()` output method can be used to perform a zone
400 budget analysis on the LAK advanced stress package using

```
401     >>> zonbud = gwf.lak.output.zonebudget(zarr)  
402     >>> zonbud.write_input()
```

```
403     >>> zonbud.run_model(silent=True)
404
405     (True, [])
406
407     zarr in the gwf.lak.output.zonebudget() is a NumPy array that defines an integer zone for
408     each lake or group of lakes in the LAK advanced stress package. Zone budget output can be
409     returned as a NumPy record array (.get_budget() or .get_volumetric_budget()) or a
410     pandas dataframe (.get_dataframes()).
```

409 Plotting

```
410     FloPy plotting capabilities have been refined and updated to support plotting both structured
411     and unstructured models in map and cross-section view using the .PlotMapView() and
412     .PlotCrossSection() classes, respectively. The plotting methods are wrappers around the
413     Matplotlib plotting methods (Hunter 2007) and allow fine-grained control using Matplotlib
414     keyword arguments (kwargs). The following Python code demonstrates the steps for plotting
415     a map of simulated heads, the model grid, the location of drain (DRN) package cells,
416     specific-discharge vectors, and head contours for the gwf model.
```

```
417     mm = flopy.plot.PlotMapView(model=gwf)
418
419     mm.plot_array(head, edgecolor="0.5")
420
421     mm.plot_bc("DRN")
422
423     mm.plot_grid()
424
425     cs = mm.contour_array(head)
426
427     mm.ax.clabel(cs)
428
429     mm.plot_vector(qx, qy, normalize=True)
430
431     plt.show()
```

```
425     Figure 3A shows the outcome of the Python code demonstrated above with additional
426     geographic features and fine-grained control of grid lines, text, annotations, tick locations, and
```

427 axis labels. Results shown in Figure 3 are for a steady-state model discretized into three
428 convertible layers, with isotropic hydraulic properties, a hydraulic conductivity of 1 m/d, with
429 rivers represented as drain cells in model in layer 1, and an areal recharge rate of 0.000001
430 m/d. Figure 3B shows use of the `.plot_array()` method to create a map of the layer
431 containing the water table, drain cells where the groundwater is discharging to a river, and
432 cells where groundwater is discharging to the surface.

433 The following Python code demonstrates the steps for plotting a cross section of
434 simulated heads and the model grid for the `gwf` model along an arbitrary line defined using a
435 list of x, y coordinate pairs (tuples) defining the vertices of the line. For structured grids, cross
436 sections can also be specified along a row or column.

```
437     fx = flopy.plot.PlotCrossSection(model=gwf,  
438                                         line={"line": [(0, 42500), (186801, 42500)]})  
439     fx.plot_array(head, head=head)  
440     fx.plot_grid()  
441     plt.show()
```

442 The `head=` keyword option for the `plot_array()` method above causes the plotting routine to
443 draw and fill only the the saturated part of the model cell (determined using the simulated
444 head and cell information). Without the `head=` keyword option, the entire cell from top to
445 bottom would be color filled based on the head value. Figure 3C and D show the outcome of
446 the Python code demonstrated along cross-section lines A–A' and B–B' (shown in Figure 3A)
447 with additional fine-grained control of grid lines, text, annotations, tick locations, and axis
448 labels. Note that the color flood of head in Figure 3C and D shows that unconfined conditions
449 occur in higher elevation cells or cells adjacent to river cells.

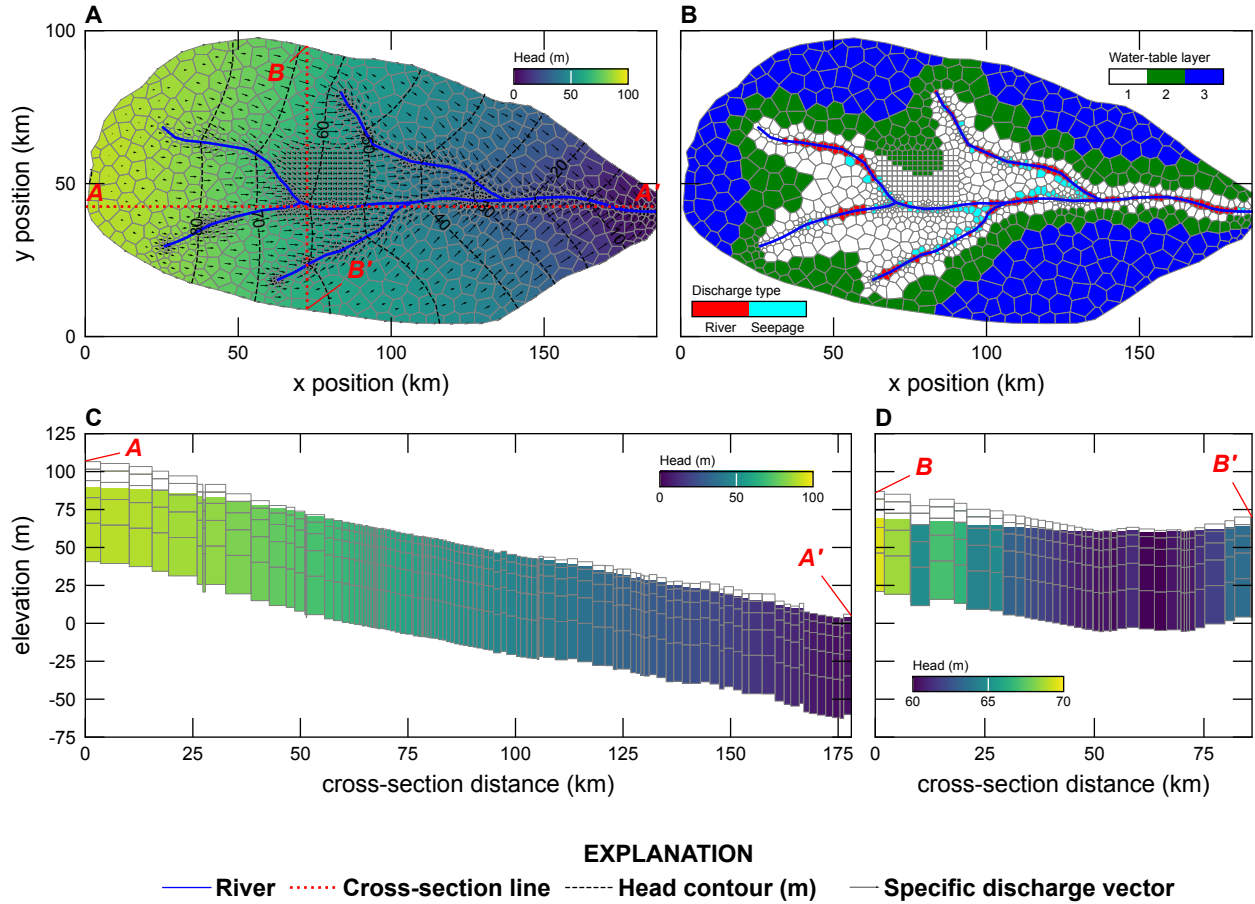


Figure 3: Examples of FloPy map and cross-section plotting capabilities for a model discretized using a Voronoi grid (Figure 1F). (A) Map showing simulated heads and specific-discharge vectors in the upper-most saturated cells. (B) Map showing the layer containing the water table, the location of cells where the aquifer is discharged to rivers represented as drain cells, and the location of cells where groundwater is discharging to the land surface (seepage). (C) East-West cross-section along line A–A', shown on Figure 3A, showing the model grid, simulated heads, and cells where water-table conditions exist. (D) North-South cross-section along line B–B', shown on Figure 3A, showing the model grid, simulated heads, and cells where water-table conditions exist.

450 Exporting Grid Data to Other Formats

451 Model input and output can be exported in a variety of standard formats using the `.export()`
 452 method, which is available for FloPy model objects, package objects, binary
 453 dependent-variable files (head, concentration, *etc.*), and cell-by-cell output files. Standard
 454 output formats that are currently supported include shapefiles ([Esri 1998](#)), NetCDF files ([Rew](#)

et al. 2006; Rew and Davis 1990), and Visualization Tool Kit (VTK) files (Schroeder et al. 2006). Entire models, packages, individual package arrays, binary dependent-variables (*e.g.*, heads), or three-dimensional representations of binary cell-by-cell data can be exported. Shapefile and VTK output can be exported for all grid types, but currently, NetCDF output can only be exported for structured grids. The NetCDF output capability has been used to convert entire models and associated output so that it can be rendered in the GWWebFlow viewer (U.S. Geological Survey 2018).

The following Python code demonstrates the steps for exporting the `gwf` model as a VTK dataset with flat cell tops and bottoms (staircase representation).

```
464     gwf.export("temp_vtk/vtk_staircase", fmt='vtk', smooth=False,  
465                 vertical_exaggeration=500.0, pvd=True)
```

VTK models can also be exported with smooth cell tops and bottoms using elevations interpolated to the cell vertices (`smooth=True`). Other supported export formats can be created by specifying the file extension to be `.shp` for shapefiles, `.nc` for NetCDF files, or if the `fmt` keyword is `vtk` (as shown above) for VTK files. Figure 4 shows staircase and smooth VTK exports of the model described in the Plotting section and rendered with ParaView (Ahrens et al. 2005).

472 Scripting MODFLOW 6 Model Development Using 473 Python and FloPy

In this section, FloPy is used to construct, run, and post process a MODFLOW 6 model. All pre- and post-processing was done using FloPy grid, geospatial processing, MODFLOW 6 processing, and plotting functionality discussed previously. Figures 5, 6, 7, and 8 were created using a combination of FloPy plotting functionality and Matplotlib plotting methods (Hunter 2007). Jupyter notebooks (Kluyver et al. 2016) showing the commands for creating the model

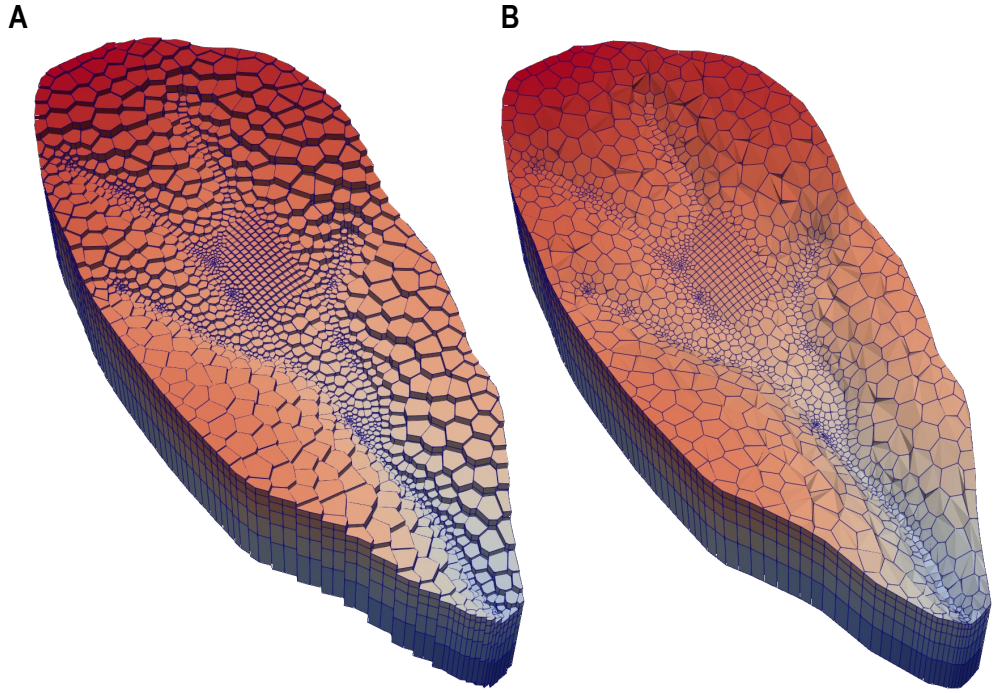


Figure 4: Two different graphical renderings of the Voronoi model grid: (A) staircase representation in which cell have flat tops and bottoms and (B) smooth representation in which elevations for cell vertices are interpolated using cell top and bottom elevations. Renderings were created using ParaView (Ahrens et al. 2005) and Visualization Tool Kit (Schroeder et al. 2006) files exported from FloPy.

479 data sets, processing model results, and plotting these figures are available at the Synthetic
480 Valley internet address indicated in the **Summary and Conclusions** section.

481 Hill et al. (1998) present a synthetic test case (Synthetic Valley) of an undeveloped
482 alluvial valley surrounded by low permeability bedrock. The model includes the Blue Lake
483 and Straight River surface water features (Figure 5A). The model in Hill et al. (1998) was
484 calibrated and simulated using MODFLOWP (Hill 1992) using a structured grid with a
485 constant 152.4 m grid spacing, three model layers, and 1,000 active cells per layer. The upper
486 two layers represent an unconfined aquifer, and the third layer represents a lower aquifer unit
487 that is separated from the overlying aquifer by a confining unit in the northern part of the
488 model domain (Figure 5A). The confining unit was not explicitly represented by Hill et al.

489 (1998); instead a quasi-3D approach (low vertical conductance) between layers 2 and 3 was
 490 used to represent the confining unit.

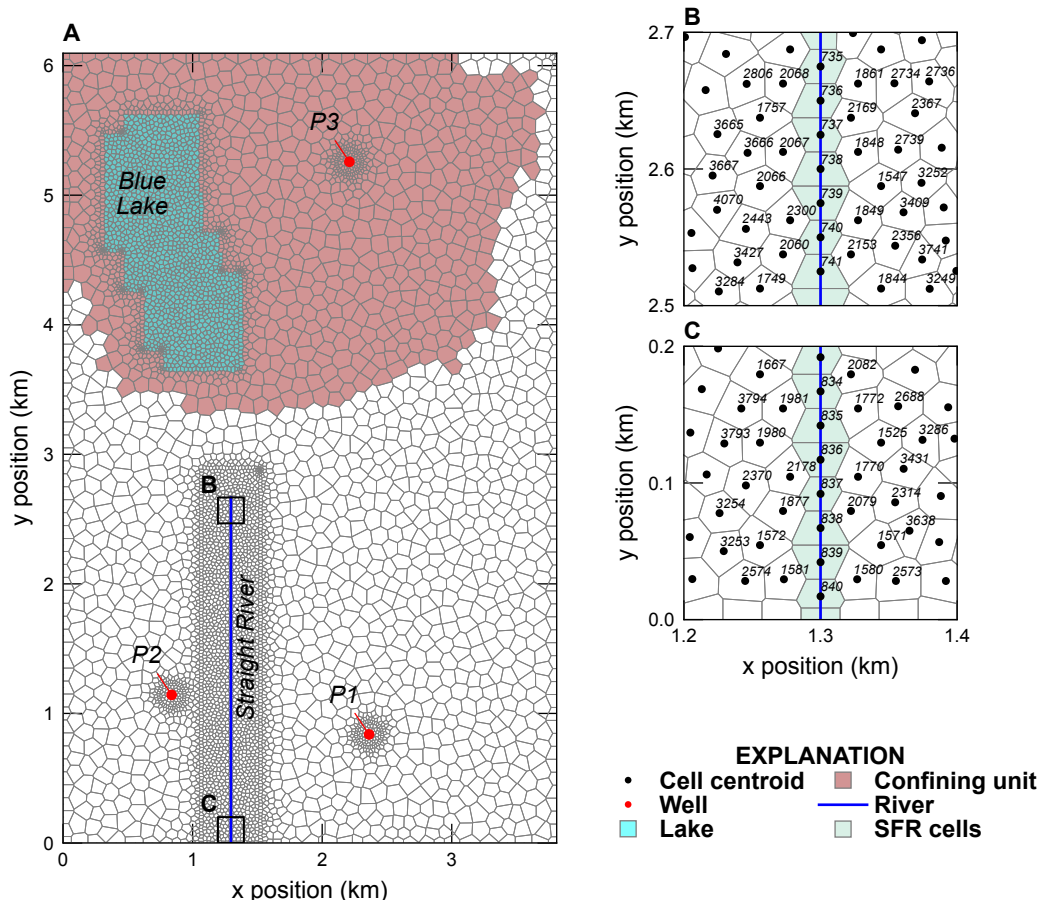


Figure 5: Synthetic Valley model used to demonstrate the MODFLOW 6 capabilities of FloPy. (A) Map showing the Voronoi grid used to discretize the model domain and the location of Blue Lake, Straight River, and the areal extent of the confining unit separating the upper and lower aquifer units. (B) Map showing model cells intersecting the northern end of Straight River. (C) Map showing model cells intersecting the southern end of Straight River. The cell centroid and cell numbers in the inset areas at the northern and southern end of Straight River are also shown on (B) and (C).

491 MODFLOW 6 Model Setup

492 To demonstrate the capabilities of FloPy and MODFLOW 6, the 6,096 m x 3,810 m model
493 domain is discretized using a Voronoi grid, with 6,343 active cells per layer, and the
494 discretization by vertices (DISV) package (Figure 5A). The model grid was developed using
495 the `Triangle()` and `VoronoiGrid()` utility classes. The model grid was refined within Blue
496 Lake, around Straight River using a 750 m buffer, and around pumping wells P1, P2, and P3
497 using a 100 m buffer.

498 In this example, both groundwater flow (Langevin et al. 2017) and solute transport
499 (Langevin et al. 2022) are simulated. To better represent solute transport, the lower aquifer
500 has been discretized into three layers (instead of one). Confining units have to be explicitly
501 simulated in MODFLOW 6, therefore, a total of six layers are simulated. The bottom of layers
502 1, 2, 3, and 4 were set to constant values of -1.53, -15.24, -15.55 and -30.48 m, respectively.
503 Model layer 3 represents the confining unit and is relatively thin (0.3 m). The `IDOMAIN`
504 concept (Langevin et al. 2017) was used to eliminate cells in model layer 3 (by setting
505 `IDOMAIN=-1`) where the confining unit does not exist. In these areas, the thickness of layer 3
506 was set to zero and `IDOMAIN` was set to -1, which marks these cells in layer 3 as “vertical pass
507 through cells” and results in cells in layer 2 being directly connected to cells in layer 4.

508 The bottom of the model (layer 6) is based on Hill et al. (1998) and the bottom of layer 5
509 was specified to be half the distance between the bottom of layers 4 and 6. The top of the
510 model was constructed from topographic contours developed for the model that was used as
511 the starting point for Hill et al. (1998) (Pollock 2014); the top of the model is shown in
512 Figure 6A. The top of the model and the bottom of layer 6 were resampled from the data used
513 in the structured grid model using the `.resample_to_grid()` method available on the
514 `VertexGrid` and linear interpolation. Figure 7 shows the vertical discretization along
515 cross-section lines A–A' and B–B', which are shown in Figure 6A.

516 Hydraulic properties for the model were resampled from the data used in the structured
517 grid model that was used as the starting point for Hill et al. (1998) (Pollock 2014). The

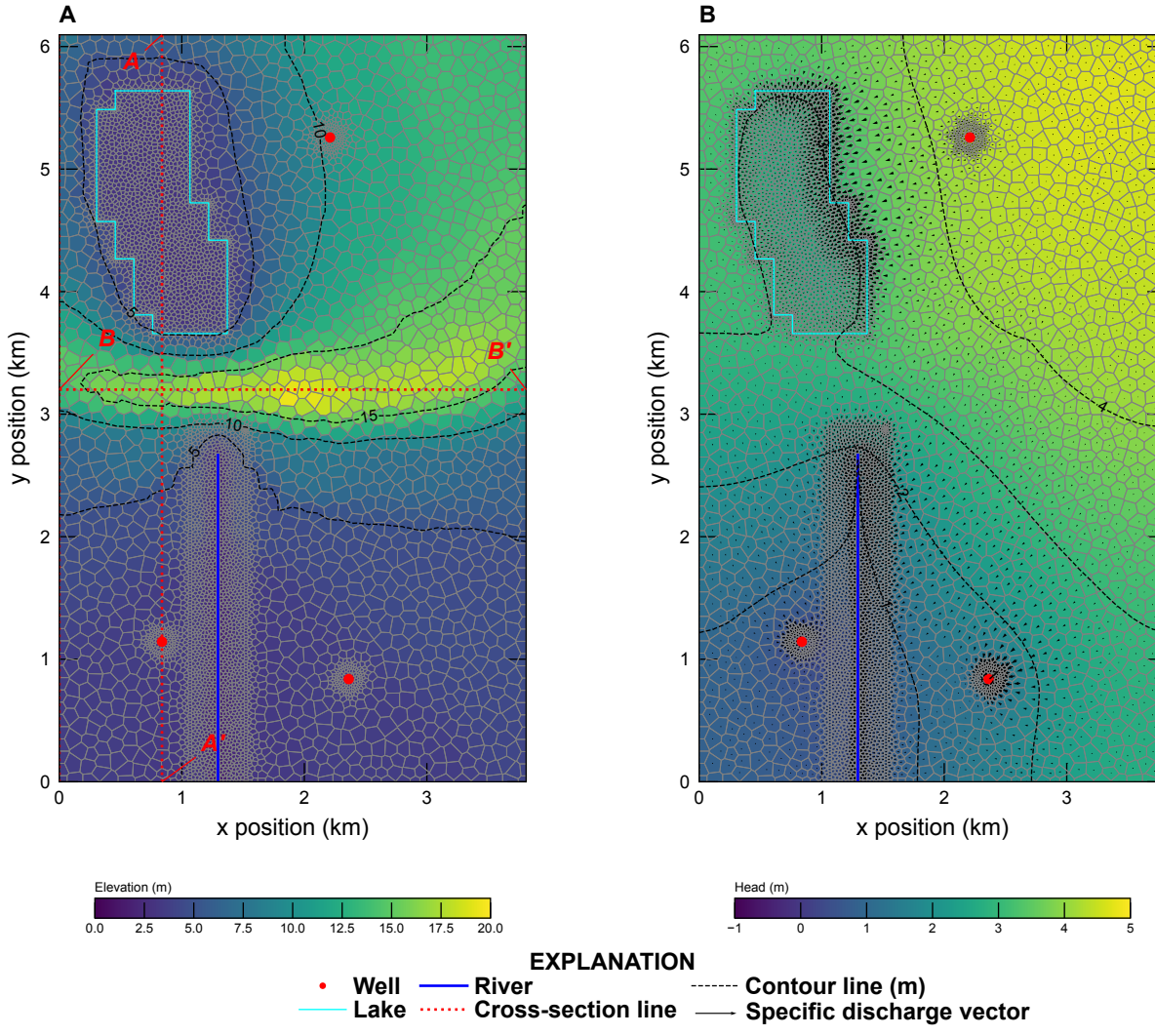


Figure 6: Map showing Synthetic Valley model (A) topography and (B) simulated steady-state heads and specific discharge rates in model layer 1. Cross-section lines A–A' and B–B' shown in Figure 7 are also shown on (A).

horizontal hydraulic conductivity was discretized into five zones with values of 45.72, 50.29, 60.96, 83.82, and 121.92 m/d; the lowest hydraulic conductivity zone was located south of Blue Lake and the highest hydraulic conductivity zone was located beneath Blue Lake. The vertical hydraulic conductivity in the upper and lower aquifer was specified to be one quarter of the horizontal hydraulic conductivity. The horizontal and vertical hydraulic conductivity in the confining unit was set equal to 9.14×10^{-4} m/d. The horizontal and vertical hydraulic conductivity were resampled from the data used in the structured grid model using the

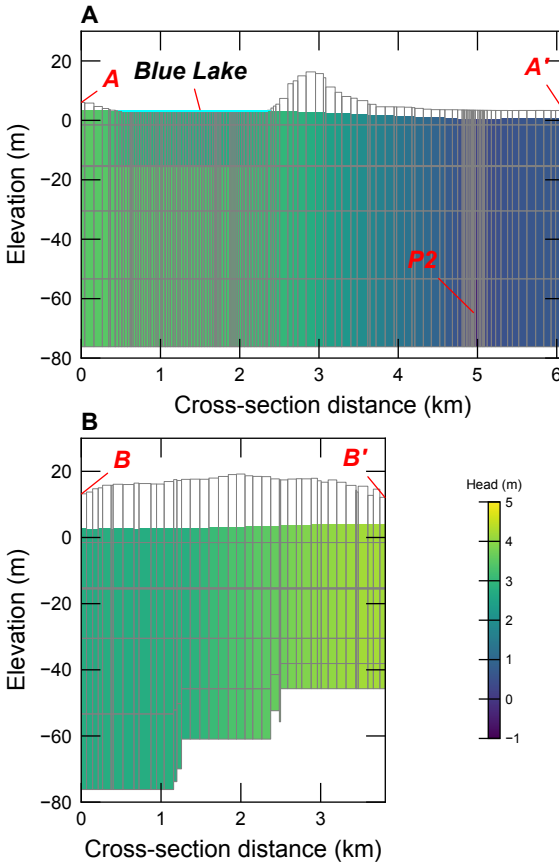


Figure 7: Cross-section of Synthetic Valley model grid and simulated steady-state heads along cross-section line (A) A–A' and (B) B–B'. The simulated Blue Lake steady-state stage (3.46 m) and pumping well P-2 are also shown on (A).

525 .resample_to_grid() method on the `VertexGrid` `modelgrid` and the nearest neighbor
 526 algorithm.

527 For the groundwater transport model, the porosity was set to 0.2 in the upper and lower
 528 aquifer and 0.4 for cells in the confining unit. For the transport model, the Total Variation
 529 Diminishing scheme available in the GWT model ([Langevin et al. 2022](#)) was used to simulate
 530 advection. Dispersion was simulated using a longitudinal dispersivity of 75 m and a transverse
 531 dispersivity of 7.5 m. Molecular diffusion was not represented.

532 In the [Hill et al. \(1998\)](#) representation of Synthetic Valley, the Straight River was

533 simulated as head-dependent river (RIV) package cells, and Blue Lake was simulated as a
534 high-hydraulic conductivity feature in model layer 1. In this recreation, Straight River is
535 simulated using the streamflow routing (SFR) package, and Blue Lake is simulated using the
536 LAK package. The SFR and LAK package cells were determined using
537 `GridIntersect().intersect()` FloPy functionality (Figure 5A).

538 Straight River was discretized into 108 SFR reaches. Cells that intersect the northern and
539 southern end of Straight River are shown in Figures 5B and C. The bed thickness and width
540 of each SFR reach was specified to be 0.3048 and 3.048 m, respectively. The leakance for each
541 SFR reach was calculated using the bed thickness, reach width, and reach length in each cell
542 and based on a total Straight River conductance of 50,971.72 m²/d. A specified rainfall rate of
543 0.0025 m/d and a potential evaporation rate of 0.0019 m/d was defined for each Straight River
544 reach.

545 Blue Lake was simulated as a lake on top of the model grid and only had vertical
546 connections to 1,406 cells in the underlying upper aquifer (model layer 1). A bed leakance of
547 0.0013 1/d was specified for each cell connected to Blue Lake. A specified rainfall rate of
548 0.0025 m/d and a potential evaporation rate of 0.0019 m/d were defined for Blue Lake.

549 Drain (DRN) cells were specified in each cell in model layer 1 that was not connected to
550 Blue Lake to prevent water levels from exceeding the top of the model. The conductance of
551 each DRN cell was based on the horizontal cell area, a thickness of 0.3048 m, and a vertical
552 hydraulic conductivity of 0.03048 m/d. Linear scaling of the drainage conductance was
553 applied to improve model convergence and ranged from 0 m²/d when groundwater levels were
554 greater than or equal to 1 m below the top of the model to the specified conductance when
555 groundwater water levels were greater than or equal to the top of the model.

556 Uniform recharge and potential evapotranspiration rates were specified using the recharge
557 (RCH) and evapotranspiration (EVT) packages, respectively, and were equal to the rates
558 specified in the SFR and LAK packages (0.0025 and 0.0019 m/d). The EVT surface was
559 specified to be the top of the model and the EVT extinction depth was specified to be 1 m.

560 The location of pumping wells P1, P2, and P3 were determined using

561 `GridIntersect().intersect()` FloPy functionality (Figure 5A). Pumping rates of -7,600,
562 -7,600, and -1,900 m³/d were specified for pumping wells P1, P2, and P3, respectively.

563 Transport was not simulated in the LAK and SFR packages. Instead, a specified
564 concentration condition with a concentration of 1.0 mg/L was specified for Blue Lake. All
565 other stress packages were assumed to have a concentration of 0 mg/L.

566 An initial head of 11 m was specified for every cell. An initial stage of 3.44 m was
567 specified for Blue Lake. An initial concentration of 0 mg/L was specified for every cell in the
568 transport model.

569 Simulated Results

570 The groundwater flow model used the Newton-Raphson Formulation with Newton
571 under-relaxation to improve convergence. The groundwater flow and transport models used
572 the Bi-conjugate Stabilized (`bicgstab`) linear accelerator and `complexity="simple"` settings.

573 The groundwater flow and transport models were run for a total of 30 years. The
574 groundwater flow model used a single steady-state time step and groundwater flow results
575 were used to run the transport model with a total of 360 time steps with a constant length of
576 30.4375 days.

577 Simulated heads and vectors of specific discharge in model layer 1 are shown in
578 Figure 6B. Specific discharge is greatest on the east side of Blue Lake and in the vicinity of
579 the three pumping wells and Straight River. Simulated heads along cross-sections A–A' and
580 B–B' are shown in Figure 7. The cross sections show that water table conditions occur in most
581 of the model domain except in the vicinity of Blue Lake.

582 Simulated concentrations at the end of 30-years in all six model layers are shown in
583 Figure 8. Simulated concentrations are highest beneath Blue Lake in model layer 1 and do not
584 vary much in model layers 1 and 2. Simulated concentrations in model layer 3 are limited to
585 the extent of the confining unit because the remaining cells in the layer are defined to be
586 vertical pass through cells (`IDOMAIN=-1`). The lateral extent of the solute plume does not vary
587 much south of Blue Lake because of the lack of confinement in these areas.

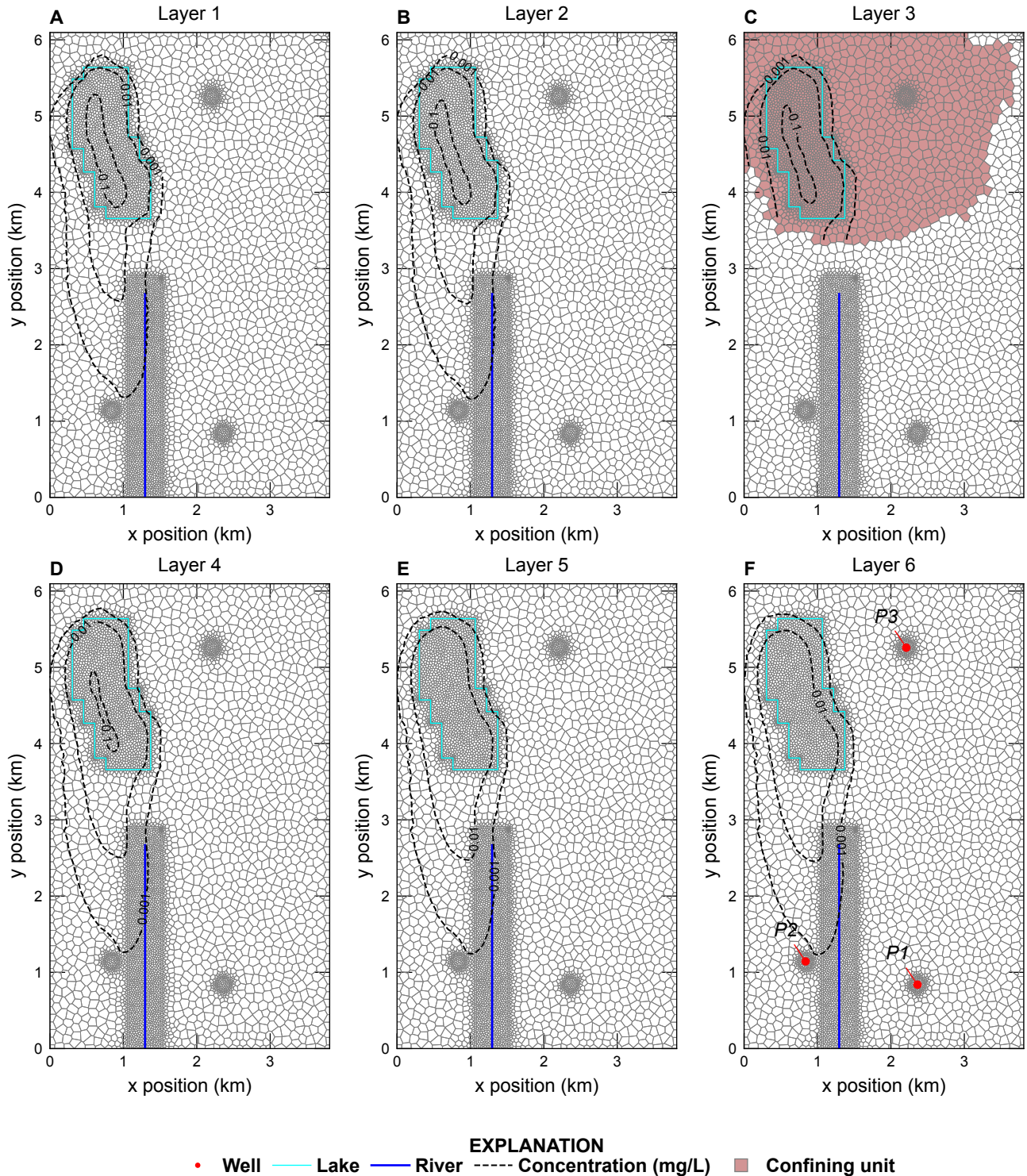


Figure 8: Maps showing Synthetic Valley simulated concentrations at the end of 30 years in model layer (A) 1, (B) 2, (C) 3, (D) 4, (E) 5, and (F) 6. The extent of the confining unit in model layer 3 is also shown on (C).

588 Summary and Conclusions

589 FloPy is a Python package for building, running, and post processing groundwater models. It
590 is open source and developed with input from a growing community of contributors. This
591 paper summarizes new FloPy capabilities that have been added since the package was first
592 described by Bakker et al. (2016). The new and updated capabilities can be summarized as
593 follows.

- 594 • FloPy supports the creation of many different types of groundwater models, including
595 models that use MODFLOW 6, MODFLOW-2005, MODFLOW-NWT,
596 MODFLOW-USG, MT3D, MT3D-USGS, and SEAWAT. FloPy support for MODFLOW
597 6 is based on an entirely new approach designed to automatically support all
598 MODFLOW 6 models, packages, and options. The underlying FloPy classes for
599 MODFLOW 6 are programmatically generated from the same input definition files that
600 are used to construct the MODFLOW 6 user guide. This correspondence ensures that
601 the FloPy classes are consistent and in-sync with MODFLOW 6 input.
- 602 • FloPy has been extended to support unstructured model grids in addition to structured
603 grids defined by layers, rows, and columns. FloPy has several different routines for
604 creating unstructured grids. FloPy includes a wrapper for the GRIDGEN program (Lien
605 et al. 2014), which can be used to create layered quadtree grids. FloPy also includes a
606 wrapper for the Triangle program (Shewchuk 1996), which can be used to create
607 triangular meshes. A triangular mesh can be converted by FloPy into a Voronoi grid.
608 Grid information is stored for each FloPy model created by the user. This model grid
609 object is used systemically throughout FloPy for geospatial operations, plotting, and
610 exporting model information to supported formats.
- 611 • Geospatial intersections of points, lines, and polygons with model grids and raster
612 resampling onto model grids are common steps in model construction. FloPy fully

613 supports these geospatial operations through its grid intersection and raster resampling
614 routines.

- 615
- 616 • Access to model output using FloPy has been simplified for MODFLOW 6 models. The
617 new output access routines makes it possible to quickly extract simulated results from
binary and text model output files.

618

 - 619 • FloPy supports plan-view map and cross-section plotting of model grids, boundary
620 conditions, and simulated results. These plotting routines work with structured and
unstructured models and can be customized to produce high quality figures.

621

 - 622 • FloPy supports the export of model information to shapefiles, VTK files, and NetCDF
623 files. These exported files can then be loaded into other software programs, such as
624 geographic information systems or advanced visualization programs for additional
processing.

625 FloPy makes it possible to construct, and reproduce the construction, of a groundwater
626 model from data in any format that can be accessed using Python. The robust new features in
627 FloPy allow users to quickly try different model grids, different model spatial and temporal
628 resolution, and different model configurations.

629 The ability to script groundwater model construction and post-processing increases
630 robustness, ensures reproducibility, provides a record of the data processing and model
631 construction steps, and provides a means to improve the model and extend the simulation
632 period as new data become available. The new geospatial processing routines make it possible
633 to change model resolution as part of the model construction script. This allows one to
634 prototype fast running models with coarse resolution and use finer resolution as the model
635 starts to behave as intended. This workflow also allows one to conduct grid convergence
636 studies to ensure that the grid is not the cause of unintended model behavior.

637 FloPy is open source and we welcome bug reports, code contributions, or improvements
638 to the documentation from the community. The FloPy Python package can be installed using

639 the `conda` or `pip` package managers. The source code, code documentation, tutorials, and
640 examples can be found in the [FloPy GitHub repository](#). The Synthetic Valley example is
641 available as a [MODFLOW 6 example](#) and the hypothetical watershed grid examples are
642 available on the [FloPy GitHub repository](#).

643 Acknowledgments

644 The authors gratefully acknowledge the efforts of Mark Bakker and Vincent E.A. Post for
645 initially developing FloPy and their continued efforts improving FloPy. Funding for this
646 research was provided by the Enterprise Capacity project of the U.S. Geological Survey
647 Integrated Water Prediction program.

648 Authors' Note

649 The authors do not have any conflicts of interest to report.

650 Disclaimer

651 Any use of trade, firm, or product names is for descriptive purposes only and does not imply
652 endorsement by the U.S. Government.

653 References

- 654 Ahrens, J., B. Geveci, and C. Law. 2005. ParaView: An End-User Tool for Large Data
655 Visualization. *Visualization Handbook*. Elsevier.
- 656 Australian Water School. 2023. On-demand: MODFLOW 6 and FloPy.
657 <https://awschool.com.au/training/modflow6-flopy/> (accessed April 13, 2023).

- 658 Bakker, M., V. Post, C.D. Langevin, J.D. Hughes, J. White, J. Starn, and M.N. Fienen. 2016.
659 Scripting MODFLOW model development using Python and FloPy. *Groundwater* 54, no. 5:
660 733–739, <https://doi.org/10.1111/gwat.12413>.
- 661 Befus, K.M., P.L. Barnard, D.J. Hoover, J.A. Finzi Hart, and C.I. Voss. 2020. Increasing
662 threat of coastal groundwater hazards from sea-level rise in California. *Nature Climate
663 Change* 10, no. 10: 946–952, <https://doi.org/10.1038/s41558-020-0874-1>.
- 664 Befus, K.M., K.D. Kroeger, C.G. Smith, and P.W. Swarzenski. 2017. The Magnitude and
665 Origin of Groundwater Discharge to Eastern U.S. and Gulf of Mexico Coastal Waters.
666 *Geophysical Research Letters* 44, no. 20: 10,396–10,406,
667 <https://doi.org/10.1002/2017GL075238>.
- 668 Burek, P., Y. Satoh, T. Kahil, T. Tang, P. Greve, M. Smilovic, L. Guillaumot, F. Zhao, and
669 Y. Wada. 2020. Development of the Community Water Model (CWatM v1.04) – a
670 high-resolution hydrological model for global and regional assessment of integrated water
671 resources management. *Geoscientific Model Development* 13, no. 7: 3267–3298,
672 <https://doi.org/10.5194/gmd-13-3267-2020>.
- 673 Ebeling, P., F. Handel, and M. Walther. 2019. Potential of mixed hydraulic barriers to
674 remediate seawater intrusion. *Science of The Total Environment* 693: 133478,
675 <https://doi.org/10.1016/j.scitotenv.2019.07.284>.
- 676 Esri. 1998. Esri Shapefile Technical Description, an ESRI white paper.
677 <http://www.esri.com/library/whitepapers/pdfs/shapefile.pdf> (accessed August 29,
678 2022).
- 679 Essawy, B.T., J.L. Goodall, W. Zell, D. Voce, M.M. Morsy, J. Sadler, Z. Yuan, and T. Malik.
680 2018. Integrating scientific cyberinfrastructures to improve reproducibility in computational
681 hydrology: Example for HydroShare and GeoTrust. *Environmental Modelling &
682 Software* 105: 217–229, <https://doi.org/10.1016/j.envsoft.2018.03.025>.

- 683 Fienen, M.N. and M. Bakker. 2016. HESS Opinions: Repeatable research: what hydrologists
684 can learn from the Duke cancer research scandal. *Hydrology and Earth System Sciences* 20,
685 no. 9: 3739–3743, <https://doi.org/10.5194/hess-20-3739-2016>.
- 686 Fienen, M.N., N.T. Corson-Dosch, J.T. White, A.T. Leaf, and R.J. Hunt. 2022. Risk-Based
687 Wellhead Protection Decision Support: A Repeatable Workflow Approach. *Groundwater* 60,
688 no. 1: 71–86, <https://doi.org/10.3389/feart.2022.903965>.
- 689 Fienen, M.N., M.J. Haserodt, A.T. Leaf, and S.M. Westenbroek. 2022. Simulation of regional
690 groundwater flow and groundwater/lake interactions in the Central Sands, Wisconsin. U.S.
691 Geological Survey Scientific Investigations Report 2022-5046, 111 p.
692 <https://doi.org/10.3133/sir20225046>.
- 693 Gillies, S. 2022. The shapely user manual.
694 <https://shapely.readthedocs.io/en/stable/manual.html> (accessed August 28, 2022).
- 695 Gillies, S. et al. 2013. Rasterio: geospatial raster I/O for Python programmers.
696 <https://github.com/rasterio/rasterio> (accessed October 6, 2022).
- 697 Guira, M. 2018. Numerical Modeling Of The Effects Of Land Use Change And Irrigation On
698 Streamflow Depletion Of Frenchman Creek, Nebraska. Master's thesis, University of
699 Nebraska, Lincoln, NE.
- 700 Hatari Labs. 2023. Regional Groundwater Modeling with MODFLOW and Flopy - Tutorial.
701 <https://hatarilabs.com/ih-en/>
702 [regional-groundwater-modeling-with-modflow-and-flopy-tutorial](https://hatarilabs.com/ih-en/regional-groundwater-modeling-with-modflow-and-flopy-tutorial) (accessed April
703 13, 2023).
- 704 Hill, M.C. 1992. A computer program (MODFLOWP) for estimating parameters of a
705 transient, three-dimensional, ground-water flow model using nonlinear regression. U.S.
706 Geological Survey Open-File Report 91-484, 358 p.

- 707 Hill, M.C., R.L. Cooley, and D.W. Pollock. 1998. A Controlled Experiment in Ground Water
708 Flow Model Calibration. *Groundwater* 36, no. 3: 520–535,
709 <https://doi.org/10.1111/j.1745-6584.1998.tb02824.x>.
- 710 Hughes, J.D., C.D. Langevin, and E.R. Banta. 2017. Documentation for the MODFLOW 6
711 framework. U.S. Geological Survey Techniques and Methods, book 6, chap. A57, 36 p.
712 <https://doi.org/10.3133/tm6A57>.
- 713 Hughes, J.D., S.A. Leake, D.L. Galloway, and J.W. White. 2022. Documentation for the
714 Skeletal Storage, Compaction, and Subsidence (CSUB) Package of MODFLOW 6. U.S.
715 Geological Survey Techniques and Methods, book 6, chap. A62, 57 p.
716 <https://doi.org/10.3133/tm6A62>.
- 717 Hunter, J.D. 2007. Matplotlib: A 2D graphics environment. *Computing in science &*
718 *engineering* 9, no. 03: 90–95.
- 719 Jaxa-Rozen, M., J.H. Kwakkel, and M. Bloemendal. 2019. A coupled simulation architecture
720 for agent-based/geohydrological modelling with NetLogo and MODFLOW. *Environmental*
721 *Modelling & Software* 115: 19–37, <https://doi.org/10.1016/j.envsoft.2019.01.020>.
- 722 Kluyver, T., B. Ragan-Kelley, F. Pérez, B. Granger, M. Bussonnier, J. Frederic, K. Kelley,
723 J. Hamrick, J. Grout, S. Corlay, P. Ivanov, D. Avila, S. Abdalla, and C. Willing. 2016.
724 Jupyter Notebooks – a publishing format for reproducible computational workflows. In
725 F. Loizides and B. Schmidt (Eds.), *Positioning and Power in Academic Publishing: Players,*
726 *Agents and Agendas*, pp. 87 – 90. IOS Press,
727 <https://doi.org/10.3233/978-1-61499-649-1-87>.
- 728 Knowling, M.J., J.T. White, and C.R. Moore. 2019. Role of model parameterization in
729 risk-based decision support: An empirical exploration. *Advances in Water Resources* 128:
730 59–73, <https://doi.org/10.1016/j.advwatres.2019.04.010>.
- 731 Langevin, C.D., J.D. Hughes, A.M. Provost, E.R. Banta, R.G. Niswonger, and S. Panday.

- 732 2017. Documentation for the MODFLOW 6 Groundwater Flow (GWF) Model. U.S.
733 Geological Survey Techniques and Methods, book 6, chap. A55, 197 p.
734 <https://doi.org/10.3133/tm6A55>.
- 735 Langevin, C.D., S. Panday, and A.M. Provost. 2020. Hydraulic-Head Formulation for
736 Density-Dependent Flow and Transport. *Groundwater* 58, no. 3: 349–362.
- 737 Langevin, C.D., A.M. Provost, S. Panday, and J.D. Hughes. 2022. Documentation for the
738 MODFLOW 6 Groundwater Transport (GWT) Model. U.S. Geological Survey Techniques
739 and Methods, book 6, chap. A61, 56 p. <https://doi.org/10.3133/tm6A55>.
- 740 Larsen, J.D., A.H. Alzraiee, D. Martin, and R.G. Niswonger. 2022. Rapid Model Development
741 for GSFLOW With Python and pyGSFLOW. *Frontiers in Earth Science* 10,
742 <https://doi.org/10.3389/feart.2022.907533>.
- 743 Leaf, A.T. and M.N. Fienen. 2022. Modflow-setup: Robust automation of groundwater model
744 construction. *Frontiers in Earth Science* 10: 903965,
745 <https://doi.org/10.3389/feart.2022.903965>.
- 746 Lien, J.M., G. Liu, and C.D. Langevin. 2014. GRIDGEN Version 1.0: A computer program
747 for generating unstructured finite-volume grids. U.S. Geological Survey Open-File Report
748 2014-1109, 26 p. <https://doi.org/10.3133/ofr20141109>.
- 749 Mancewicz, L.K., A. Mayer, C.D. Langevin, and J. Gulley. 2022. Improved method for
750 simulating groundwater inundation using the MODFLOW 6 Lake Transport Package.
751 *Groundwater*, <https://doi.org/10.1111/gwat.13254>.
- 752 Mehl, S.W. and M.C. Hill. 2006. MODFLOW-2005, the U.S. Geological Survey modular
753 ground-water model-documentation of shared node local grid refinement (LGR) and the
754 boundary flow and head (BFH) package. U.S. Geological Survey Techniques and Methods,
755 book 6, chap. A12, 78 p. <https://doi.org/10.3133/tm6A12>.

- 756 Mehl, S.W. and M.C. Hill. 2013. MODFLOW-LGR—Documentation of ghost node local grid
757 refinement (LGR2) for multiple areas and the boundary flow and head (BFH2) package.
758 U.S. Geological Survey Techniques and Methods, book 6, chap. A44, 43 p.
759 <https://doi.org/10.3133/tm6A44>.
- 760 Morway, E.D., C.D. Langevin, and J.D. Hughes. 2021. Use of the MODFLOW 6 water mover
761 package to represent natural and managed hydrologic connections. *Groundwater* 59, no. 6:
762 913–924, <https://doi.org/10.1111/gwat.13117>.
- 763 Panday, S., C.D. Langevin, R.G. Niswonger, M. Ibaraki, and J.D. Hughes. 2013.
764 MODFLOW-USG version 1—An unstructured grid version of MODFLOW for simulating
765 groundwater flow and tightly coupled processes using a control volume finite-difference
766 formulation. U.S. Geological Survey Techniques and Methods, book 6, chap. A45, 66 p.
- 767 Perry, M. 2013. Rasterstats python library.
768 <https://github.com/perrygeo/python-rasterstats>.
- 769 Pollock, D.W. 2014. Personal communication. Reston, VA.
- 770 Provost, A.M., C.D. Langevin, and J.D. Hughes. 2017. Documentation for the “XT3D”
771 Option in the Node Property Flow (NPF) Package of MODFLOW 6. U.S. Geological Survey
772 Techniques and Methods, book 6, chap. A56, 46 p. <https://doi.org/10.3133/tm6A56>.
- 773 Rew, R. and G. Davis. 1990. NetCDF: an interface for scientific data access. *IEEE computer
774 graphics and applications* 10, no. 4: 76–82.
- 775 Rew, R., E. Hartnett, J. Caron, et al. 2006. NetCDF-4: Software implementing an enhanced
776 data model for the geosciences. In *22nd International Conference on Interactive
777 Information Processing Systems for Meteorology, Oceanograph, and Hydrology*, Volume 6.
- 778 Rossetto, R., G. De Filippis, I. Borsi, L. Foglia, M. Cannata, R. Criollo, and E. Vázquez-Suñé.
779 2018. Integrating free and open source tools and distributed modelling codes in GIS

- 780 environment for data-based groundwater management. *Environmental Modelling &*
781 *Software* 107: 210–230, <https://doi.org/10.1016/j.envsoft.2018.06.007>.
- 782 Schroeder, W., K. Martin, and B. Lorensen. 2006. *The Visualization Toolkit* (4th ed.).
783 Kitware.
- 784 Shewchuk, J.R. 1996. Triangle: Engineering a 2D Quality Mesh Generator and Delaunay
785 Triangulator. In *Applied Computational Geometry, Towards Geometric Engineering,*
786 *FCRC'96 Workshop, WACG'96, Philadelphia, PA, USA, May 27-28, 1996, Selected Papers*,
787 pp. 203–222. <https://doi.org/10.1007/BFb0014497>.
- 788 Starn, J.J. and K. Belitz. 2018. Regionalization of Groundwater Residence Time Using
789 Metamodeling. *Water Resources Research* 54, no. 9: 6357–6373,
790 <https://doi.org/10.1029/2017WR021531>.
- 791 Sun, A.Y. 2018. Discovering State-Parameter Mappings in Subsurface Models Using
792 Generative Adversarial Networks. *Geophysical Research Letters* 45, no. 20: 11,137–11,146,
793 <https://doi.org/10.1029/2018GL080404>.
- 794 U.S. Geological Survey. 2018. GWWebFlow—a browser-based groundwater model viewer.
795 <https://webapps.usgs.gov/gwwebflow/>.
- 796 van Engelen, J., G.H. Oude Essink, H. Kooi, and M.F. Bierkens. 2018. On the origins of
797 hypersaline groundwater in the Nile Delta aquifer. *Journal of Hydrology* 560: 301–317,
798 <https://doi.org/10.1016/j.jhydrol.2018.03.029>.
- 799 Vilhelmsen, T.N., S. Christensen, and S.W. Mehl. 2012. Evaluation of MODFLOW-LGR in
800 connection with a synthetic regional-scale model. *Groundwater* 50, no. 1: 118–132,
801 <https://doi.org/10.1111/j.1745-6584.2011.00826.x>.
- 802 Virtanen, P., R. Gommers, T.E. Oliphant, M. Haberland, T. Reddy, D. Cournapeau,
803 E. Burovski, P. Peterson, W. Weckesser, J. Bright, S.J. van der Walt, M. Brett, J. Wilson,
804 K.J. Millman, N. Mayorov, A.R.J. Nelson, E. Jones, R. Kern, E. Larson, C.J. Carey,

- 805 İ. Polat, Y. Feng, E.W. Moore, J. VanderPlas, D. Laxalde, J. Perktold, R. Cimrman,
806 I. Henriksen, E.A. Quintero, C.R. Harris, A.M. Archibald, A.H. Ribeiro, F. Pedregosa,
807 P. van Mulbregt, and SciPy 1.0 Contributors. 2020. SciPy 1.0: Fundamental Algorithms for
808 Scientific Computing in Python. *Nature Methods* 17: 261–272,
809 <https://doi.org/10.1038/s41592-019-0686-2>.
- 810 White, J.T. 2018. A model-independent iterative ensemble smoother for efficient
811 history-matching and uncertainty quantification in very high dimensions. *Environmental
812 Modelling & Software* 109: 191–201, <https://doi.org/10.1016/j.envsoft.2018.06.009>.
- 813 White, J.T., L.K. Foster, M.N. Fienen, M.J. Knowling, B. Hemmings, and J.R. Winterle.
814 2020. Toward reproducible environmental modeling for decision support: A worked
815 example. *Frontiers in Earth Science* 8: 50, <https://doi.org/10.3389/feart.2020.00050>.
- 816 Zhou, Z. and D.M. Tartakovsky. 2021. Markov chain Monte Carlo with neural network
817 surrogates: application to contaminant source identification. *Stochastic Environmental
818 Research and Risk Assessment* 35, no. 10: 639–651,
819 <https://doi.org/10.1007/s00477-020-01888-9>.
- 820 Zipper, S.C., T. Gleeson, B. Kerr, J.K. Howard, M.M. Rohde, J. Carah, and J. Zimmerman.
821 2019. Rapid and Accurate Estimates of Streamflow Depletion Caused by Groundwater
822 Pumping Using Analytical Depletion Functions. *Water Resources Research* 55, no. 7:
823 5807–5829, <https://doi.org/10.1029/2018WR024403>.

824 Figure captions

825	1	Examples of grids that can be generated and processed using FloPy for a hypothetical watershed, including (A) a structured MODFLOW grid with constant and equal row and column spacings, (B) a structured MODFLOW grid with variable row and column spacings, (C) a structured MODFLOW child grid nested within a structured MODFLOW parent grid, (D) a quadtree grid generated with the GRIDGEN program (Lien et al. 2014) through the FloPy wrapper, (E) a triangular grid generated with the Triangle program (Shewchuk 1996) through the FloPy wrapper, and (F) a Voronoi grid created from the triangular mesh. All of the grids have refinement in the location of the child grid in (C).	8
834	2	Examples of the intersection of a linear stream network with the model grids shown in Figure 1. Intersections were performed using FloPy for (A) a structured MODFLOW grid, (B) a structured MODFLOW grid with variable row and column spacing, (C) a structured MODFLOW child grid nested within a structured MODFLOW parent grid, (D) a quadtree grid, (E) a triangular grid, and (F) a Voronoi grid. Shaded cells represent those cells that intersect with the linear stream network.	15
841	3	Examples of FloPy map and cross-section plotting capabilities for a model discretized using a Voronoi grid (Figure 1F). (A) Map showing simulated heads and specific discharge vectors in the upper-most saturated cells. (B) Map showing the layer containing the water table, the location of cells where the aquifer is discharged to rivers represented as drain cells, and the location of cells where groundwater is discharging to the land surface (seepage). (C) East-West cross-section along line A–A', shown on Figure 3A, showing the model grid, simulated heads, and cells where water-table conditions exist. (D) North-South cross-section along line B–B', shown on Figure 3A, showing the model grid, simulated heads, and cells where water-table conditions exist.	21

851	4	Two different graphical renderings of the Voronoi model grid: (A) staircase representation in which cell have flat tops and bottoms and (B) smooth representation in which elevations for cell vertices are interpolated using cell top and bottom elevations. Renderings were created using ParaView (Ahrens et al. 2005) and Visualization Tool Kit (Schroeder et al. 2006) files exported from FloPy.	23
852			
853			
854			
855			
856	5	Synthetic Valley model used to demonstrate the MODFLOW 6 capabilities of FloPy. (A) Map showing the Voronoi grid used to discretize the model domain and the location of Blue Lake, Straight River, and the areal extent of the confining unit separating the upper and lower aquifer units. (B) Map showing model cells intersecting the northern end of Straight River. (C) Map showing model cells intersecting the southern end of Straight River. The cell centroid and cell numbers in the inset areas at the northern and southern end of Straight River are also shown on (B) and (C).	24
857			
858			
859			
860			
861			
862			
863			
864	6	Map showing Synthetic Valley model (A) topography and (B) simulated steady-state heads and specific discharge rates in model layer 1. Cross-section lines A–A' and B–B' shown in Figure 7 are also shown on (A).	26
865			
866			
867	7	Cross-section of Synthetic Valley model grid and simulated steady-state heads along cross-section line (A) A–A' and (B) B–B'. The simulated Blue Lake steady-state stage (3.46 m) and pumping well P-2 are also shown on (A).	27
868			
869			
870	8	Maps showing Synthetic Valley simulated concentrations at the end of 30 years in model layer (A) 1, (B) 2, (C) 3, (D) 4, (E) 5, and (F) 6. The extent of the confining unit in model layer 3 is also shown on (C).	30
871			
872			